Nanoscale

Optical identification of layered MoS$_2$ via characteristic matrix method

Yuanxin Li, Ningning Dong, Saifeng Zhang, Kangpeng Wang, Long Zhang, Jun Wang†

Key Laboratory of Materials for High-Power Laser, Shanghai Institute of Optics and Fine Mechanics, Chinese Academy of Sciences, Shanghai 201800, China.

†Corresponding Author: jwang@siom.ac.cn

Abstract

It is demonstrated that the characteristic matrix method is effective and reliable for the optical identification of two-dimensional layered nanomaterials on different substrates. By using this method, the authors calculate the reflectivity and optical contrast of layered MoS$_2$ crystallites prepared on quartz by chemical vapor deposition. It is found that the measured pixel intensity of MoS$_2$ optical image under continuous spectrum light is proportional to the calculated reflectivity, and that the theoretical optical contrast agrees well with the experimental results. This work provides a new way for the calculation of the optical contrast of the 2D nanomaterials and layered heterostructures on various substrates.

1. Introduction

A primary condition for devices and properties research based on two-dimensional (2D) materials,[1] e.g., graphene,[2] transition metal dichalcogenides (TMDs),[3-7] black phosphorus,[8] etc., is that these materials should be able to be visualized on a substrate using optical microscopy (OM).[9] In Ref. [10], H. Li et al. proposed a rapid and reliable method to identify the thickness of 2D nanosheets using OM. They have successfully distinguished the maximum number of layers up to 10 of 2D nanomaterials including graphene, MoS$_2$, WSe$_2$, etc. on SiO$_2$/Si using a simple OM method. In Ref. [11], H.C. Wang et al. reported an optical detection method based on the multispectral imaging technology to identify the number of large-area graphene film layers. This method is substrate-independent and can be used to distinguish the graphene layers on glass that cannot be identified using OM. These experimental methods are committed to the rapid identification of the thickness of 2D materials on different substrates and beneficial to their basic and applied research in many fields. On the other hand, many theoretical calculations for the optical contrast of graphene,[9] MoS$_2$,[12] and graphene/MoS$_2$ heterostructures[13] on SiO$_2$/Si have been performed by using the Fresnel theory.[9, 12-17] These studies provide a guide for the selection of the illumination wavelength or the substrates when observing the 2D materials using OM.[9] However, the Fresnel theory calculations become complicated and time-consuming when the number of layers of 2D materials is increased.[12, 13, 16] In this work, we demonstrate that the characteristic matrix method can be used to calculate the optical contrast of 2D layered MoS$_2$ on different substrates. By using this method, we obtained color contour plots of the optical contrast as a function of both the MoS$_2$ layer number and the incident light wavelength. In addition, the reflectivity and optical contrast of MoS$_2$ under continuous spectrum light were calculated, and the results

agree well with the directly measured values from the OM images.

2. Experimental section

In this study, MoS$_2$ with different layers on SiO$_2$/Si and quartz were synthesized through chemical vapor deposition (CVD) method, the details of which are the same with our previous research.[18] The characterization measurements including OM images, Raman and photoluminescence (PL) spectra were carried out using a confocal microscopy system (Monovista-P optical workstation). The OM images (Figs. 1 (a) and (d)) were captured by a digital camera (Suntime500A) of the microscopy (Olympus BX53) with a 100× objective lens (NA = 0.9) under a continuous spectrum light (halogen non-reflector lamps, Philips 7724 100W GY6.35 12V 1CT), which has a color temperature of 3100 K and the chromaticity coordinates of (0.479, 0.435). The spectrum of this light source (Fig. 3 (c)) was measured using the "Ocean Optics HR4000CG-UV-NIR" spectrometer with a variable-blazed grating. The digital camera of the OM has effective pixels of 2592H*1944V with 10 bit, and the dynamic range is ~ 60 dB with the signal to noise ratio of 40 dB. Under these conditions, the minimum lateral size of MoS$_2$ single crystal that can be distinguished is ~ 1 μm. The size of the OM images in this work is 2591*1944, and the optical contrast of these images were measured using ImageJ (version 1.46p, National Institute of Health, USA).[10]

In the Raman and PL measurements, the excitation laser is a LD pumped 532 nm continuous laser with output power of 2 mW. Considering that ~ 10 % laser irradiated on the surface of MoS$_2$ and the diameter of laser spot was ~ 1μm, the incident laser intensity was deduced to be ~ 254.6 μW/μm^2, which is sufficiently low not to cause any local heating during the Raman and PL measurements.[19] The Raman and PL signals were measured at room temperature by Acton Princeton Instruments SP2500 imaging spectrograph with a grating of 1200 g/mm and a thermoelectric cooled CCD at -75 ℃. In addition, the images of MoS$_2$ on SiO$_2$/Si were captured by field-emission scanning electron microscopy (FE-SEM, Auriga, Carl Zeiss).

3. Results and discussion

Figures 1 (a) and (d) show the typical OM images of the MoS$_2$ with different layers on 300 nm SiO$_2$/Si and 1 mm quartz, respectively. It is clearly seen that the optical contrast of the red and black arrow directed domains in Fig. 1 (a) are different due to the fact that the two triangle domains have a different number of layers. Figures 1 (b) and (c) show the SEM images of the MoS$_2$ on SiO$_2$/Si. Compared with the region indicated by the red arrow in Fig. 1 (b), the black arrow directed region in Fig. 1 (c) shows a fluctuation in surface morphology because of the deposition of multilayers during the growth progress. These MoS$_2$ multilayers cannot be distinguished clearly using SEM, but similar structures are recognizable using OM, as shown in Figs. 1 (d). R0 represents the surface of the quartz, and R1–R4 signify regions with different layers of MoS$_2$, respectively. It can be easily seen by naked eyes that the color and brightness of R0–R4 are different. To quantize the difference, we used ImageJ to measure the pixel intensity (I$_{exp}$) along the two arrows in Fig. 1 (d). As shown in Fig. 1 (e), both measured I$_{exp}$ curves along the two arrows from region 1 to 4 increase in a step-type manner. The corresponding experimental optical contrast (C$_{exp}$) can be defined as:[9]

$$C_{exp} = \frac{I_{exp}(MoS_2) - I_{exp}(substrate)}{I_{exp}(substrate)} \tag{1}$$

The red dash lines in Fig. 1 (e) indicate that the two arrows crossed regions possess approximately the same optical contrast; the values are summarized in Fig. 1 (f) and Table 1. For instance, the I_{exp} of R1 is 35.42, and the corresponding C_{exp} is 0.7781. It should be pointed out that the orange curve crossed R4 region has a saturation because the reflected light intensity was over the dynamic range of the digital camera. This saturation results in the maximum number of MoS_2 layers that can be identified in our work only reaches up to 4 using this OM method. In this study, we also measured the optical contrast of MoS_2 on SiO_2/Si (Fig. S1 (a)). The results indicate the MoS_2 on SiO_2/Si has negative optical contrast ($I_{exp}(MoS_2) < I_{exp}(substrate)$) in comparison with that of the sample in Fig. 1 (d), which leads to the fact that the surface of the thick MoS_2 looks darker than the substrate and the thin MoS_2 for samples on SiO_2/Si, while it is brighter for samples on quartz. It is also found that MoS_2 on SiO_2/Si (Fig. S1 (b)) prepared by other method[20] has this feature as well, and the details are described in the supplementary information (SI). That is to say, the species of substrates can have an influence on the optical contrast of 2D nanomaterials. In addition, it should be pointed out that the optical contrast is affected by the gap between the 2D materials and the substrate. As the transferred MoS_2 shown in Fig. S1 (c), the optical contrast has an obvious reduction due to the large gap.
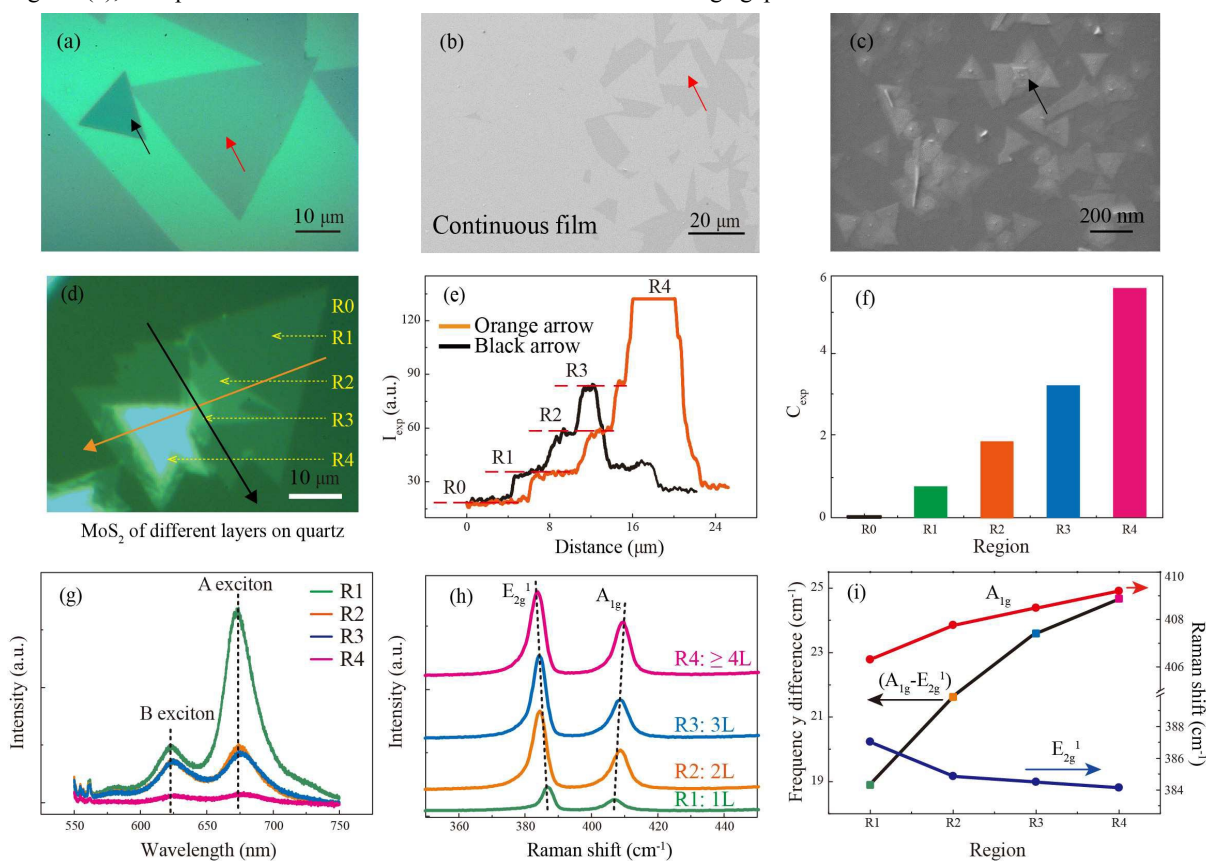
Fig. 1 (a) OM image of MoS_2 with different thicknesses (indicated by red and black arrow) on SiO_2/Si; (b) SEM image of continuous MoS_2 film with triangular domain (red arrow) at the edge; (c) SEM image of stacked MoS_2 multilayers (black arrow); (d) OM image of MoS_2 with different layers on transparent quartz; R0-R4 represent the quartz surface, 1-3 and ≥4 layers of MoS_2, respectively; (e) measured pixel intensity along the two arrows in (d) (the flat peak of the orange curve is due to the fact that the I_{exp} of region 4 exceeds the dynamic range of the digital camera); (f) C_{exp} of R0–R4; (g) PL of R1–R4 with A and B exciton transition peaks; (h) Raman spectra of R1-R4 with E_{2g}^1 and A_{1g} modes; (i) the Raman shift of two modes and the frequency differences between the two modes.

To clarify the relationship between the C_{exp} (Fig. 1 (f)) and the MoS_2 layer number, we carried out the PL and

Raman spectra measurement of R1–R4 to identify the corresponding layers. As shown in Fig. 1 (g), the PL spectra of R1-R3 have two obvious peaks located at ~670 nm and ~625 nm corresponding to the A and B exciton transition,[21] whereas R4 scarcely shows any signal owing to the thicker layers. The PL intensity decreases rapidly from R1 to R4, indicating that the layer number increases due to the layer dependent PL property of MoS_2.[21] Figure 1 (h) shows the Raman spectra of the four regions with two characteristic bands corresponding to the in-plane (E_{2g}^1) and out-of-plane (A_{1g}) vibrational modes.[22] It can be seen that the E_{2g}^1 mode peak position has an obvious red shift while the A_{1g} mode has a blue shift from region 1 to 4 which means the increasing of the layer number. The variation of the two modes and the frequency difference between them are shown in Fig. 1 (i); it can be seen that the frequency differences are ~18.9, ~21.4, ~23.3, and ~24.5 cm^{-1} for R1–R4, respectively. Due to the fact that the frequency difference between E_{2g}^1 mode and A_{1g} mode is a reliable quantity to distinguish the number of MoS_2 layers on different substrates,[23] we concluded that the corresponding estimated layer number is 1, 2, 3 and ≥4 for R1–R4 based on the previous study.[22-24] Based on these results, the specific correspondence between C_{exp} and the MoS_2 layer number is summarized in Table 1.

Table 1. Measured and calculated optical contrast and reflectivity for R0–R4.

Region	MoS_2 layer number	I_{exp} (a.u.)	C_{exp}	R_{theor}	C_{theor} (N_{bulk})	Relative error (%, N_{bulk})	C_{theor} (N_{1L})	Relative error (%, N_{1L})
R0	0	19.92	0	0.0348	0	0	0	0
R1	1	35.42	0.7781	0.0626	0.7972	~ 2.45	0.7659	~ 1.57
R2	2	57.67	1.895	0.1045	2.0020	~ 5.65	2.0517	~ 8.23
R3	3	84.72	3.2529	0.1534	3.4050	~ 4.68	3.5949	~ 10.52
R4	≥4	132.07	N/A	N/A	N/A	N/A	N/A	N/A

In order to calculate the optical contrast of the sample shown in Fig. 1 (d) under continuous spectrum light, we propose the characteristic matrix method for the first time. By using this method, we first calculate the optical contrast of both graphene and MoS_2/graphene heterostructures on SiO_2/Si, and demonstrate its feasibility by comparing with the reported results.[8, 12,17] The theoretical optical contrast is usually defined as the relative intensity of reflected light in the presence ($N_2 \neq 1$) and absence ($N_2 = N_1 = 1$) of 2D materials on a substrate.[9] According to this definition, the optical contrast of the monolayer graphene on SiO_2/Si (Fig. 2 (a)) can be written as[9, 15, 16]

$$C_{theor} = \frac{R(n_1=1) - R(n_1)}{R(n_1=1)},$$ (2)

where R (n_1=1) and R (n_1) correspond to the reflectivity of the substrate and monolayer graphene, respectively, and N_2 is the complex refractive index (2.6-1.3j) of the monolayer graphene. The graphene combined with the SiO_2/Si substrate constitutes a film system (G/SiO_2/Si), the reflectivity of which can be written as

$$R(\lambda) = r \cdot r^* = \left(\frac{\eta_0 - Y}{\eta_0 + Y}\right) \cdot \left(\frac{\eta_0 - Y}{\eta_0 + Y}\right)^*,$$ (3)

where r is the complex reflection coefficient, and η_0 is n_0 for the normal incident light. Y denotes the equivalent optical conductance of the film system and can be calculated using the formula Y=C/B, where B and C can be written as

$$\begin{bmatrix} B \\ C \end{bmatrix} = \left\{ \Pi_{j=1}^k \begin{bmatrix} cos\delta_j & \frac{i}{\eta_j} sin\delta_j \\ i\eta_j sin\delta_j & cos\delta_j \end{bmatrix} \right\} \begin{bmatrix} 1 \\ \eta_{k+1} \end{bmatrix}.$$ (4)

The right side of Eq. 2 is the characteristic matrix of the G/SiO_2/Si system, where $\delta_j = 2\pi N_j d_j$, and $\eta_j = N_j$ assuming normal incident.
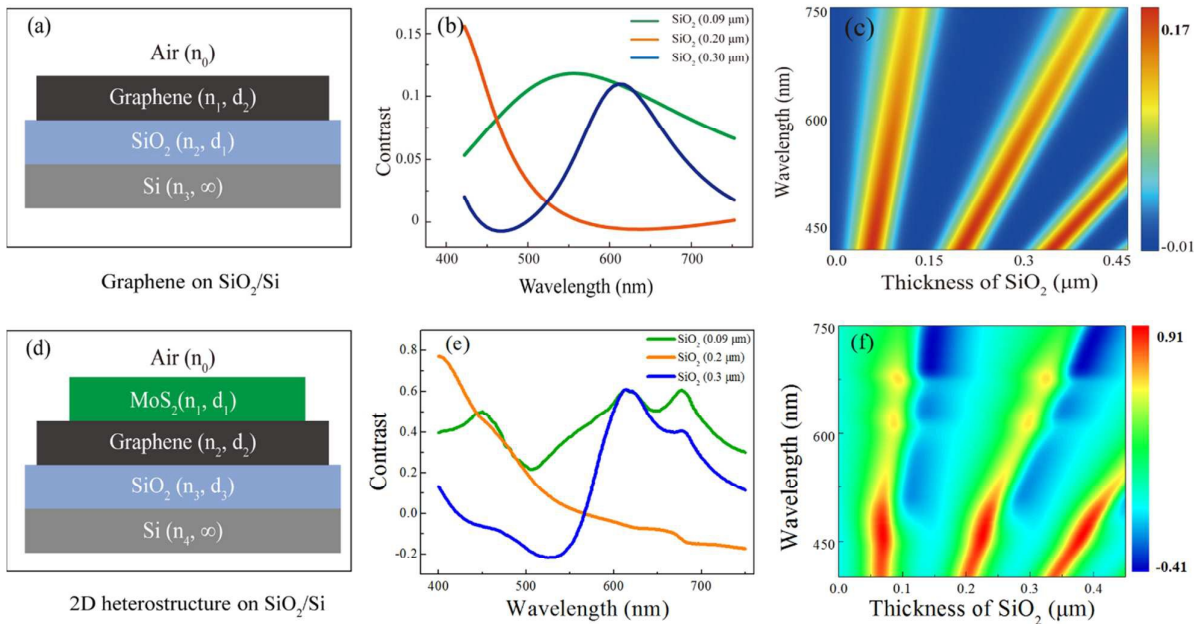
Fig. 2 (a) Schematic of the $G/SiO_2/Si$ system, and the thickness of Si (∞) is much larger than that of the other layers; (b) calculated contrast of the monolayer graphene on SiO_2/Si for SiO_2 of the thickness 0.09, 0.2, 0.3 μm; (c) color counter plot of the contrast as a function of the thickness of SiO_2 and incident wavelength; (d) schematic of the $MoS_2/G/SiO_2/Si$ film system; (e) calculated contrast of the $MoS_2/G/SiO_2/Si$ system for SiO_2 of the thickness 0.09, 0.2, 0.3 μm; (f) color counter plot of the contrast as a function of the thickness of SiO_2 and incident wavelength for the $MoS_2/G/SiO_2/Si$.

Using Eqs. (2), (3) and (4), we calculated the contrast of the $G/SiO_2/Si$ system with SiO_2 thickness of 0.09, 0.2 and 0.3 μm. As shown in Fig. 2 (b), the contrast peaks reach up to the values of ~0.12 and ~0.1 for SiO_2 of thickness 0.09 and 0.3 μm, respectively, which are consistent with the experimental results (~0.125 and ~0.095) and are better than the theoretical fitting data via the Fresnel Formula reported in Ref. [7]. As for the substrate with SiO_2 of thickness 0.2 μm, the contrast increases gradually with the decrease in the incident wavelength with slight vibration at short wavelengths compared with the previous study, which may be due to the fact that the parameters (e.g. the refractive index of SiO_2 and Si) used for calculations are not completely identical. Furthermore, the optical contrast variation with the incident wavelength and the thickness of SiO_2 was also calculated (Fig. 1 (c)), and the result was in good agreement with the previous study.[9]

It should be realized that every matrix in parenthesis of Eq. 3 is the characteristic matrix of the corresponding layer of the film system, and this matrix determines the light propagation property of this layer. If the layers of the film system increase or the film system is a 2D heterostructure as shown in the Fig. 2 (d), we just need to multiply the corresponding characteristic matrix of these layers to obtain the characteristic matrix of the entire film system without increasing the computation workload (Eq. S11), which makes this method appropriate for calculating the contrast of the multilayers and the heterostructures. As shown in Figs. 2 (e) and (f), we simulated the optical contrast variation of the $MoS_2/G/SiO_2/Si$ heterostructure along with the incident wavelength and thickness of the SiO_2. The peak of the contrast reaches up to 0.6 for the substrate with SiO_2 of thickness 0.09 and 0.3 μm at ~620 nm, which is consistent with the reported results in Ref. [9]. It should be mentioned that we used the wavelength-dependent bulk MoS_2 complex refraction index to calculate the optical contrast of the heterostructure. More comparative results were shown in Fig. S2 after considering the difference between the monolayer and the bulk MoS_2.[17] All these theoretical analysis confirm that the characteristic matrix method is effective and reliable for optical contrast calculation of the 2D nanomaterials and the

corresponding heterostructures. In addition, the characteristic matrix method is a theory of stratified media (multilayer),[25] based on Maxwell's equation, which has taken account the infinite number of reflections between two adjacent interfaces including the destructively or constructively interfere.[25, 26] From this point, the characteristic matrix method is more accurate and convenient to calculate the reflectivity and optical contrast of multilayers than Fresnel equations, which is based on a single interface and becomes complicate and cumbersome for multiple interfaces.[26]
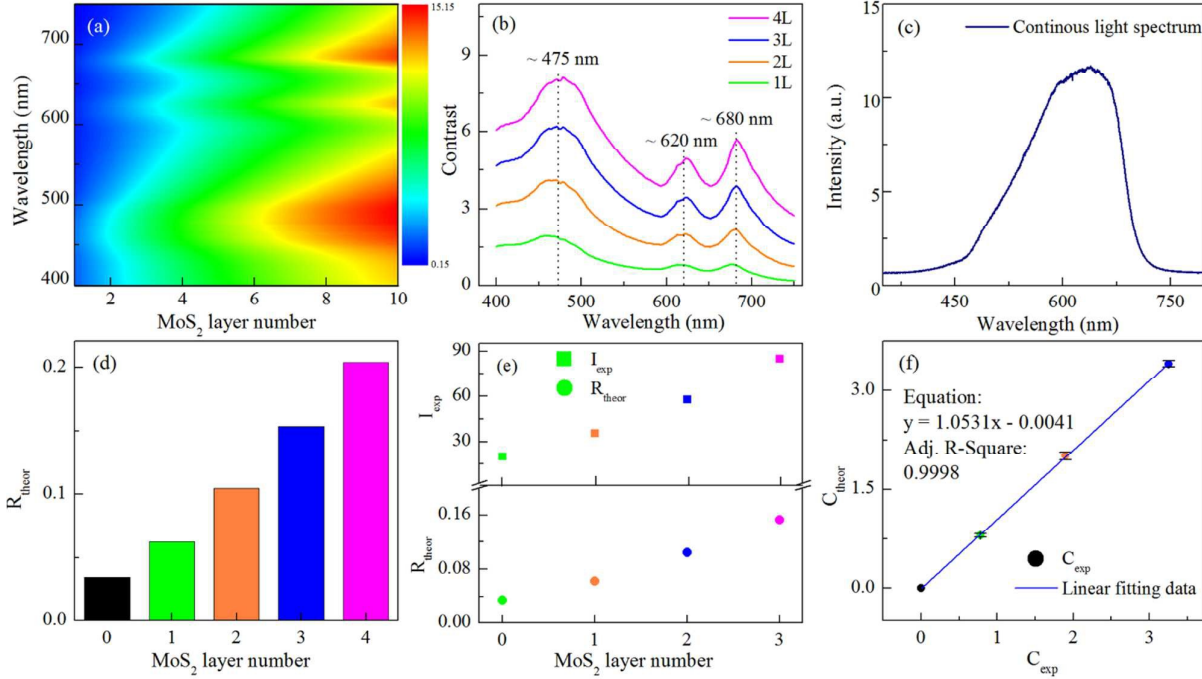
Fig. 3 (a) Color counter plot of the contrast as a function of the layer number of MoS$_2$ and the incident wavelength; (b) wavelength-dependent contrast of 1–4 layers of MoS$_2$ on quartz; (c) continuous spectrum light spectrum for capturing all the OM images in this work; (d) calculated reflectivity of 0–4 layers of MoS$_2$; (e) compare plots between the measured OM pixel intensity and calculated reflectivity of 0-3 layers of MoS$_2$; (f) linear fitting of C$_{exp}$ and C$_{theor}$ illustrates the proportional relationship between them.

We used the characteristic matrix method to calculate the optical contrast of MoS$_2$ with different layers on quartz. The details of the calculation were discussed in the SI. As shown in Fig. 3 (a), we determine the color contour plot of the optical contrast as a function of the MoS$_2$ layer number and incident light wavelength. The result illustrates that the theoretical contrast increases with the increases in the layer number for a specific wavelength. Figure 3 (b) shows the calculated reflectivity of 1–4 layers MoS$_2$ as a function of wavelength. It can be seen that there are three peaks of the optical contrast for 1-4L MoS$_2$ on quartz, which can be attributed to the fact that the real and imaginary part of the complex refractive index have three peaks at the corresponding positions (Fig. S2 (a)). Based on this result, one can choose ~ 475, 620, 680 nm light source as illuminant for better observation of MoS$_2$ on quartz using OM. Both Figs. 3 (a) and (b) illustrate that the MoS$_2$ with more layers shows larger optical contrast, which is consistent with the experimental results as shown in Fig. 2 (f). In order to calculate the optical contrast of MoS$_2$ on quartz (Fig. 2 (d)) under continuous spectrum light, we first measured the continuous spectrum (S (λ), Fig. 3 (c)) and used Eq. (5) to calculate the reflectivity of 0–4 layers of MoS$_2$ under the measured spectrum.[12]

$$R = \frac{\int_{\lambda=400\,nm}^{\lambda=750\,nm} S(\lambda) \cdot R(\lambda) d\lambda}{\int_{\lambda=400\,nm}^{\lambda=750\,nm} S(\lambda) d\lambda} \tag{5}$$

The calculated reflectivity (R$_{theor}$) are shown in Fig. 3 (d), and it is found that the R$_{theor}$ of quartz and monolayer MoS$_2$

on quartz under continuous spectrum light are 3.48 % and 6.26 %, respectively. The R_{theor} for the other layers are summarized in Table 1. To compare the measured I_{exp} with the R_{theor}, we plotted them as a function of MoS_2 layer number, as shown in Fig. 3 (e). Moreover, it is observed that the I_{exp} is directly proportion to the R_{theor} as shown in the Fig. S3. The result is reasonable because that the I_{exp} is the manifestation of the reflected light, which is proportional to the R_{theor}. In addition, we also obtained the theoretical optical contrast (C_{theor}) by using Eqs. (2) and (5), and its relationship with C_{exp} is shown in Fig. 3 (f). The linear fitting result shows that C_{exp} is equal to ($1.0531 * C_{theor} - 0.0041$) having an adjusted coefficient of determination (Adj. R-Square) ~0.9998. This result confirms the proportional relationship between the measured optical contrast and theoretical optical contrast. Note, however, the ration relationship is not of the same size, which could be attributed to deviations from normal light incidence and the admissible error in the measurement.[9] It should be pointed out that in the above calculation, we used the wavelength-dependent complex refractive index of bulk (N_{bulk}) MoS_2 (Fig. S2 (a)). In fact, the complex refractive index of monolayer MoS_2 (N_{1L}) is different from that of the bulk[17]. To make comparison, we also calculated the optical contrast of MoS_2 using N_{1L}, and the results are shown in Table 1 and Fig. S4. The relative error is obtained from $|C_{exp} - C_{theor}|/C_{exp}$. It can be seen that for monolayer MoS_2, the relative error calculated using N_{1L} (~ 1.57%) is smaller than the one deduced using N_{bulk} (~ 2.45%); but for 2 and 3 layer MoS_2, the relative errors calculated using N_{1L} increase rapidly (2L: ~ 8.23%, 3L: ~ 10.52%), and they are larger than those deduced using N_{bulk} (2L: ~ 5.65%, 3L: ~ 4.68%). These results illustrate that the complex refractive indexes of 2-3 layer MoS_2 are also different from that of the monolayer, which means MoS_2 probably has a layer-dependent refractive index from monolayer to bulk. The calculation details of this part are summarized in the SI.

In summary, we have investigated the optical contrast of MoS_2 with different layers on quartz grown by chemical vapor deposition. By calculating the visibility of $G/SiO_2/Si$ and $MoS_2/G/SiO_2/Si$, we have demonstrated that the characteristic method is effective and reliable for the optical contrast calculation. The experimental results and theoretical analysis confirm the linear relationship between the pixel intensity of OM images (measured optical contrast) and reflectivity of MoS_2 (theoretical contrast) under continuous spectrum light. Our study provides a new train of thought for detecting 2D materials and heterostructures on top of various substrates by using the characteristic matrix method.

Reference

1   K. S. Novoselov, V. I. Fal'ko, L. Colombo, P. R. Gellert, M. G. Schwab and K. Kim, *Nature*, 2012, **490**, 192-200.

2   K. S. Novoselov, A. K. Geim, S. V. Morozov, D. Jiang, M. I. Katsnelson, I. V. Grigorieva, S. V. Dubonos and A. A. Firsov, *Nature*, 2005, **438**, 197-200.

3   Q. H. Wang, K. Kalantar-Zadeh, A. Kis, J. N. Coleman and M. S. Strano, *Nat. Nanotechnol*, 2012, **7**, 699-712.

4   K. P. Wang, J. Wang, J. T. Fan, M. Lotya, A. O'Neill, D. Fox, Y. Y. Feng, X. Y. Zhang, B. X. Jiang, Q. Z. Zhao, H. Z. Zhang, J. N. Coleman, L. Zhang and W. J. Blau, *Acs Nano*, 2013, **7**, 9260-9267.

5   S. Zhang, N. Dong, N. McEvoy, M. O'Brien, S. Winters, N. C. Berner, C. Yim, Y. Li, X. Zhang, Z. Chen, L. Zhang,

G. S. Duesberg and J. Wang, *ACS Nano*, 2015, **9**, 7142-7150.

6   X. Zou, Y. Leng, Y. Li, Y. Feng, P. Zhang, Y. Hang and J. Wang, *Chin. Opt. Lett.*, 2015, **13**, 081405-081408.

7   G. Z. Wang, S. F. Zhang, X. Y. Zhang, L. Zhang, Y. Cheng, D. Fox, H. Z. Zhang, J. N. Coleman, W. J. Blau and J. Wang, *Photonics Research*, 2015, **3**, A51-A55.

8   X. Wang, A. M. Jones, K. L. Seyler, V. Tran, Y. Jia, H. Zhao, H. Wang, L. Yang, X. Xu and F. Xia, *Nat. Nanotechnol*, 2015, **10**, 517-521.

9   P. Blake, E. W. Hill, A. H. Castro Neto, K. S. Novoselov, D. Jiang, R. Yang, T. J. Booth and A. K. Geim, *Appl. Phys. Lett.*, 2007, **91**, 063124.

10   H. Li, J. Wu, X. Huang, G. Lu, J. Yang, X. Lu, Q. Xiong and H. Zhang, *ACS Nano*, 2013, **7**, 10344-10353.

11   H. C. Wang, S. W. Huang, J. M. Yang, G. H. Wu, Y. P. Hsieh, S. W. Feng, M. K. Lee and C. T. Kuo, *Nanoscale*, 2015, **7**, 9033 – 9039.

12   M. M. Benameur, B. Radisavljevic, J. S. Heron, S. Sahoo, H. Berger and A. Kis, *Nanotechnol.*, 2011, **22**, 125706.

13   H. Xu, D. He, M. Fu, W. Wang, H. Wu and Y. Wang, *Opt. Express*, 2014, **22**, 15969-15974.

14   A. Castellanos-Gomez, N. Agrait and G. Rubio-Bollinger, *Appl. Phys. Lett.*, 2010, **96**, 213116.

15   M. Friedemann, K. Pierz, R. Stosch and F. J. Ahlers, *Appl. Phys. Lett.*, 2009, **95**, 102103.

16   E. B. Song, B. Lian, G. Y. Xu, B. Yuan, C. F. Zeng, A. Chen, M. S. Wang, S. Kim, M. R. Lang, Y. Zhou and K. L. Wang, *Appl. Phys. Lett.*, 2010, **96**, 081911.

17   H. Zhang, Y. Ma, Y. Wan, X. Rong, Z. Xie, W. Wang and L. Dai, *Sci Rep*, 2015, **5**, 8440.

18   Y. X. Li, N. N. Dong, S. F. Zhang, X. Y. Zhang, Y. Y. Feng, K. P. Wang, L. Zhang and J. Wang, *Laser Photonics Rev.*, 2015, **9**, 427-434.

19   S. Najmaei, Z. Liu, P. M. Ajayan and J. Lou, *Appl. Phys. Lett.*, 2012, **100**, 013106.

20   I. Bilgin, F. Liu, A. Vargas, A. Winchester, M. K. L. Man, M. Upmanyu, K. M. Dani, G. Gupta, S. Talapatra, A. D. Mohite and S. Kar, *ACS Nano*, 2015, **9**, 8822-8832.

21   A. Splendiani, L. Sun, Y. Zhang, T. Li, J. Kim, C. Y. Chim, G. Galli and F. Wang, *Nano Lett*, 2010, **10**, 1271-1275.

22   C. Lee, H. Yan, L. E. Brus, T. F. Heinz, J. Hone and S. Ryu, *ACS Nano*, 2010, **4**, 2695-2700.

23   M. Buscema, G. A. Steele, H. S. J. van der Zant and A. Castellanos-Gomez, *Nano Research*, 2015, **7**, 561-571.

24   H. Li, Q. Zhang, C. C. R. Yap, B. K. Tay, T. H. T. Edwin, A. Olivier, D. Baillargeat, *Adv. Funct. Mater.* 2012, **22**, 1385–1390

25   M. Born, E. Wolf, Principles of optics: electromagnetic theory of propagation, interference and diffraction of light, 1964, Page 54.

26   https://en.wikipedia.org/wiki/Transfer-matrix_method_(optics)